136 *KSME International Journal, Vol. 11, No. 2, pp. 136~142, 1997*

Experimental Investigation on Low Energy Impact Behavior of Foam Cored Sandwich Composites

S. H. Yoon*, Y. W. Kwon and L. A. Clawson, Jr.****

(Received May 11, 1996)

This study focuses on an experimental investigation of damage tolerance of the foam cored sandwich composite subjected to low energy impact. Tests are performed to correlate delamination length with failure loads and loss of damage tolerance of the sandwich composite. The impact force history is used to determine momentum imparted to the specimen, the work done on the specimen, and the kinetic energy in order to gain an understanding of the mechanisms involved in damage due to impact loading.

Key Words: Foam Cored Sandwich Composite, Delamination, Damage Tolerance, Low Energy Impact, Impact Force History, Momentum, Kinetic Energy

1. Introduction

A sandwich composite consists of two faceplates adhesively bonded to a lightweight inner core. The faceplates carry principal loads while the inner core acts to transmit the shear load between the faceplates. Applications of sandwich composites include the space shuttle, remote piloted vehicle (RPV) aircraft, small boats, etc.

Much of the recent focus on the selection of the sandwich composites has been on using graphite/epoxy or fiberglass/epoxy faceplates with various types of honeycomb or lightweight foam material for the core (Johnson and Sims, 1986). One of the major concerns in using sandwich composites is the loss of load-carrying capability that may be induced in the event of delamination between the faceplates and the inner core. Delamination may occur due to a number of factors such as low energy impact, manufacturing defects, and high stress concentrations at geometric and/or material discontinuities. Delamination may occur unknowingly and limit the load-carrying capability of the sandwich composites severely. Knowledge of the damage tolerance is necessary to allow engineers to determine what degree of impact, if any, can be allowed in the service life of the sandwich composites.

Within the past decade, most of the work has centered on the impact damage and response of laminate composites, but sandwich composites have recently been receiving growing attention. In Sjoblöm, Hartness and Cordell (1988) it is reported that during low energy impact testing, the initial potential energy of the impactor is not enough to predict the impact behavior, but that the impact response of the specimen depends on geometry, material properties, and impactor velocity. It is further reported that the impact loadcell for the detection of damage works very well as long as the damage results in a fast, large load drop. Crane and Juska (1989) suggest that impact force history may be used to determine the level of force, displacement, and energy at which major damage is initiated. By plotting impact energy loss versus initial impact energy of the impactor, it is reported that damage by delamination is reflected by an abrupt increase in impact energy loss at a specific level of initial impact energy, and matrix cracks are found within the

* Department of Mechanical Engineering, Kumoh National University of Technology, Kumi, Kyungbuk, 730-701, Korea

** Mechanical Engineering Department, Naval Postgraduate School, Monterey, CA 93943, USA

specimen subjected to impact energy below the level which results in damage by delamination. Kim and Jun (1992) have shown that the energy that is not converted to elastic deformation is absorbed by the specimen as permanent deformation such as core crushing and shear deformation. Work by Nemes and Simmonds (1992) has shown that, for impact conditions producing displacements larger than $1/100^{th}$ the faceplate thickness, the contact deformation of fully intact sandwich composites is dominated by the core rather than by the faceplate. The most prevalent damage of foam cored sandwich composites appears to occur at the interface between the faceplates and core. The impact damage is also driven predominantly by the excessive transverse shear stress resulting from the impact. As plastic deformation and small scale matrix cracking cannot be detected by observing the force versus time history, Carlyle and Adler (1984) have shown that acoustic emission sensors can be used to detect and measure the early onset of matrix cracking. Most studies examine the failure modes, including delamination, of the composite materials, but very little literature exists on studying the effects of pre-existing large scale delaminations.

The primary focus of this study is an experimental investigation of the damage tolerance of foam cored symmetric sandwich composites subjected to impact. Different specimens, each having a different core thickness, are tested to determine the effect of core thickness on impact behavior. Furthermore, specimens with various delamination lengths between the faceplate and core are tested to determine the effect of delamination on the damage tolerance of foam cored sandwich composites. The impact force history is used to develop equations for the momentum imparted to the specimen, the work done on the specimen, and the kinetic energy to aid in understanding the mechanisms involved in damage due to impact.

2. Specimen Preparation

Figure 1 shows the configuration of the sandwich composite specimen used for this study. The

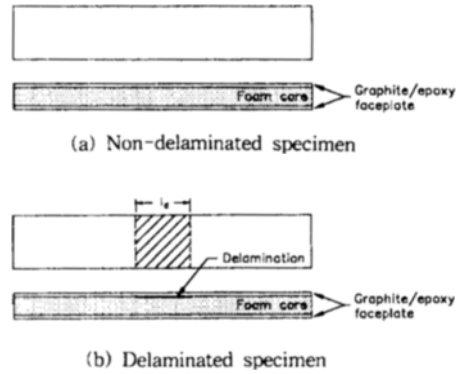

Fig 1. Configuration of sandwich composite specimen.

specimens are a symmetric sandwich composite with top and bottom faceplates of $[0_2/90_2/0_2]$ graphite/epoxy and an inner core of rohacell polymethacrylimide rigid foam. The term 'symmetric' refers to the fact that the two faceplates are of identical material and thickness. All of the test specimens are 381mm in length and 38.1mm in width and the faceplates are nominally 0.96mm in thickness. The core thicknesses of the specimens are varied to observe the effect of core thickness on impact behavior, at thicknesses of 3mm, 6.35mm, and 12.7mm. The specimens were made from manufacturer's specifications. During the manufacturing process, Teflon film with 0.025mm thickness was inserted to create the initial delamination between the faceplate and core. The width of delamination was 38.1mm, so delamination ran across the full width of the specimen. The longitudinal lengths of delamination varied from 12.7mm, 25.4mm, 50.8mm, 101.6mm, to 152.4mm. The specimen had a delamination located on only one side of the specimen. Impact tests were performed in an ambient temperature of 20 ± 3℃ with an average relative humidity of 40 ± 8%.

3. Experimental Apparatus

A weight drop impact tower was designed to conduct the impact tests. The impact tower in Fig. 2 consists of a sliding impactor guided by four stainless steel guide rods and associated structural

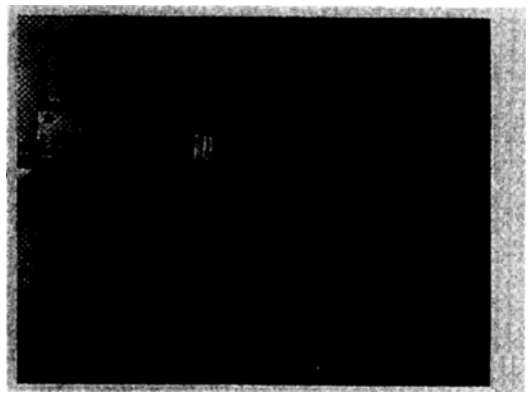

Fig 2. Overview of impact test set-up.

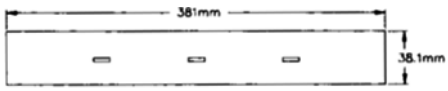

(a) Bottom view

(b) Side view

Fig 3. Strain gage placements.

supports. Precision linear bearing pillow blocks were used for the sliding friction between the impactor and guide rods, and the resulting sliding friction between the impactor and guide rods was negligible. The mass of the impactor may easily be varied by the addition or removal of specially designed weights. All tests during this study were performed with an impactor weight of either 21. 7N or 50.7N. The drop heights varied from 12. 7mm to 940mm. A test fixture, solidly fastened to the impact tower structure, held the specimen in the simply supported condition snugly. The fixture prevented lateral and vertical motion of the specimen-support contact points during impact. The specimen was aligned on the support fixture to ensure the impactor head strike the center of the specimen. A thin strip of brass, 69.8mm×69. 8mm×1.52mm, was secured to the center of that the impacted faceplate to spread the load over the width of the specimen.

The actual impactor, attached to the sliding mass assembly, had a PCB piezotronics force transducer Model 200A04 with a calibration range of 4448N. The impact force transducer was powered by a PCB piezotronics Model 482 voltage power supply. The test specimens were instrumented with five CEA-13-250UN-350 strain gages (Micro Measurements Inc.) mounted longitudinally and centered on the width of the specimen. Two strain gages were placed at the quarter length on the impacted faceplate and three strain gages were placed on the opposite side. Figure 3 shows the strain gage placements. The strain gages were connected to an Ectron amplifier bridge Model E513-6A-M997. The five strain gage outputs and the impact force transducer output were each assigned a channel on an analog to digital computer board in an IBM PC with a data acquisition program.

4. Data Reduction Procedures

The impact energy was varied for each impact test by varying the drop height. In performing a series of impact tests on any given specimen, the drop weight was kept fixed while the dropheight was incrementally increased until an indication of damage was detected. Any drop in load versus time or an abrupt change in strain versus time was taken as an indication of damage.

The force history was used to determine energies, acceleration, velocity, and distance versus time for the impact event. The impact force measured by the force transducer is the actual force applied to the specimen during the impact event. Theacceleration of theimpactor isobtained from Newton's second law

$$mg-F=ma \tag{1}$$

where F is the force applied to the specimen read from the force transducer and mg is the gravitational force of the impactor.

Equation (1) may be rearranged to solve for the acceleration of the impactor during the impact event by considering the weight of the impactor, W

$$a=\left[1-\left(\frac{F}{W}\right)\right]g \tag{2}$$

whereby the acceleration of the impactor is determined each time the impact force is measured. For this study, a sampling frequency of 4000Hz was used; thus the force and strain data were sampled every 0.25msec.

Equating the initial potential energy of the impactor before release with the kinetic energy at impact, the initial velocity of the impactor at the instant of impact becomes

$$v=\sqrt{2gh} \tag{3}$$

The impactor velocity at any time during the impact event may be determined from the previous velocity and the average acceleration during the sampling time interval, $[t_{i-1}, t_i]$. The velocity is obtained by

$$v_i=v_{i-1}+\frac{(a_{i-1}+a_i)}{2}dt \tag{4}$$

where dt is the time interval between sampling points.

The displacement of the impactor during the impact event is obtained in a similar manner by

$$s_i=s_{i-1}+\frac{(v_{i-1}+v_i)}{2}dt \tag{5}$$

The kinetic energy absorbed by the specimen during the impact event, taken to be the loss in kinetic energy of the impactor, is then determined by

$$t_i=t_{i-1}+\frac{1}{2}m(v_i^2{}_{-1}\ v_i^2) \tag{6}$$

Furthermore, the work done on the specimen and momentum imparted to the specimen during the impact event are determined from

$$W=\int fds \tag{7}$$

$$M=\int fdt \tag{8}$$

5. Experimental Results

Impact tests were conducted on all non-delaminated and delminated specimens. The original intent for this study was to begin impact testing on any given specimen with small energy impact and to subsequently increase the impact energy until an indication of damage was detected. The damage would be manifested in a sudden drop of the impact force or sudden change on the strain-time curve of the impat event due to the brittleness of the specimen. Such brittleness characteristics were reflected in the specimens absorbing all of the energy of impact elastically until the impact energy was suffcient to cause catastrophic failure. No specimens displayed any visual signs of damage at any impact energy below the level which caused catastrophic failure.

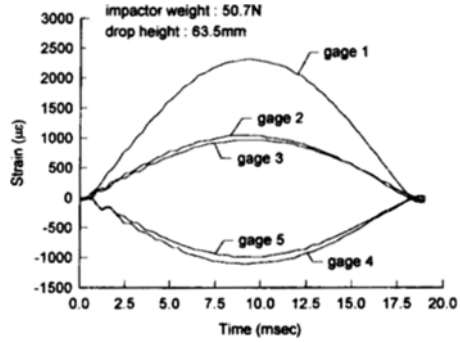

Fig 4. Impact strains versus time for 12.7mm core thickness with non-delamination in case of no failure.

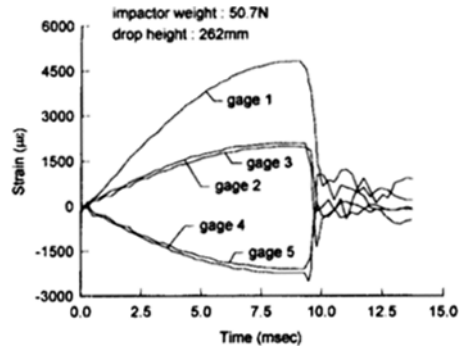

Fig 5. Impact strains versus time for 12.7mm core thickness with non-delamination in case of no failure.

Figure 4 depicts a typical strain versus time trend for impact tests where failure did not occur. The relatively smooth trace of the impact strain indicates that no damage occurred. Figure 5 reveales a typical failure event. Note the sudden change in resulting strain. For a specimen repeatedly impacted without failure, the maximum strain on impact would increase with increasing drop height. For all specimens except

for the 152.4mm delaminated ones, the absolute strains at the quarter points on the impact faceplate were very nearly equal to those at the quarter points on the faceplate opposite to the impact side.

Tables 1 through 3 list force and strain measurements for the failure event of each specimen.

For non-delaminated specimens, the maximum strain at failure varied only from 2014~2565 $\mu\varepsilon$ even though the core thickness of the specimen varied from 3mm to 12.7mm. The failure mode of the non-delaminated specimens was failure by core shear. Impact on the non-delaminated side of the delaminated specimens caused failure at much lower peak force and strain for 50.8mm, 101.6mm, and 152.4mm delamination than those for non-delaminated specimens. The failure mode for the delaminated specimens impacted on the non-delaminated side was failure by delamination spreading for the 101.6mm and 152.4mm delaminated specimens and by core shear with attendant delamination for the specimens with other sizes of delamination. The 12.7mm delaminated specimen actually had a higher maximum force of impact than did the non-delaminated specimen. For the delaminated side impact, force and strain trends were very similar to those of the non-delaminated side impact. The maximum force of the delaminated side impact was about 60% that of the non-delaminated side impact for the 50.8mm, 101.6mm, and 152.4mm delaminated specimens. The maximum force of the 25.4mm delaminated specimen was nearly equal. For the 12.7mm delaminated specimen, the maximum force of the delaminated side impact was only 72% that of the non-delaminated side impact. The failure mode for the delaminated side impact was always core shear originating at the edge of delamination.

Table 1. Impact response for the non-delaminated specimens.

Core thickness (mm)	Weight(N)/ Height(mm)	Failure force (N)	Max. quarter point strain($\mu\varepsilon$)	Max. mid-point strain($\mu\varepsilon$)
3.0	50.7/203	564.5	2565	5448
6.35	21.7/686	979.5	2310	5470
6.35	50.7/228	1128.0	2353	5766
12.7	50.7/262	1807.3	2014	4876

Table 2. Impact response on non-delaminated side for the delaminated specimens.

Delamination length(mm)	Weight(N)/ Height(mm)	Failure force (N)	Max. quarter point strain($\mu\varepsilon$)	Max. mid-point strain($\mu\varepsilon$)
152.4	21.7/25	161.5	721	2078
101.6	21.7/51	277.6	594	2226
50.8	21.7/203	613.8	1696	3752
25.4	21.7/660	943.0	2374	5766
12.7	21.7/838	1209.9	2396	5576

Table 3. Impact response on delaminated side for the delaminated specimens

Delamination length(mm)	Weight(N)/ Height(mm)	Failure force (N)	Max. quarter point strain($\mu\varepsilon$)	Max. mid-point strain($\mu\varepsilon$)
152.4	21.7/25	102.3	1548	1569
101.6	21.7/25	169.5	445	1887
50.8	21.7/76	379.8	996	2714
25.8	21.7/609	922.5	2247	5576
12.7	21.7/686	877.6	2247	5809

Figures 6 and 7 showed the duration of various impact events. For the non-delaminated specimens, the impact duration increased with decreasing core thickness. The varying impact time for different core thickness was deemed to be a function of the global stiffness of the specimen. The specimens with thicker cores, having a larger

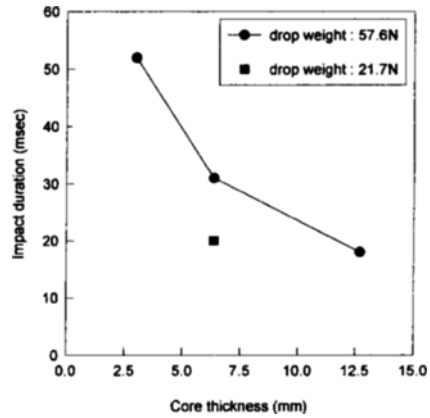

Fig 6. Variation of impact duration with core thickness and drop weight.

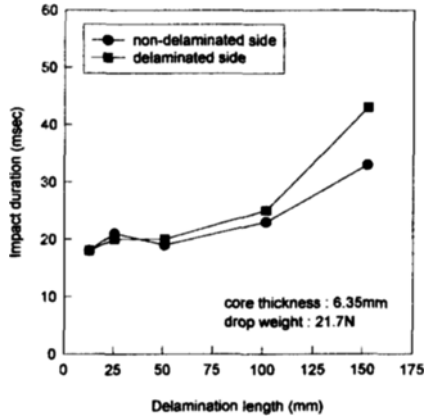

Fig 7. Impact duration of the delaminated specimens with various delamination lengths.

cross-sectional area, had a higher global stiffness and released the bending strain energy resulting from the impact faster than those with thinner cores. The impact duration increased with increasing drop weight until failure. For the delaminated specimens, the 152.4mm delaminated specimen impacted on the non-delaminated side had a duration 23% shorter than the duration of the specimen impacted on the delaminated side. For other delamination lengths, the impact duration increased as the length of delamination increased. This is in agreement with the above discussion, as the increased length of delamination causes a decrease in the stiffness of the specimen.

The force history for each impact event was used to calculate the momentum imparted to the specimen, the work done on the specimen by the impactor, and the kinetic energy as shown in Eqs. (6) through (8). Table 4 shows the impact energies of failure event for the non-delaminated specimens. To observe failure differences with varying drop weight, drop height, and velocity, the non-delaminated specimen with 6.35mm core thickness was impacted with 50.7N and 21.7N at heights such that in the two tests have the same potential energy at the impactor's release. The lower weight impact required a higher drop height to induce failure than did the test with the heavier drop weight. Tables 5 and 6 showed that

Table 4. Impact energies of failure event for the non-delaminated specimens.

Core thickness (mm)	Weight(N)/ Height(mm)	Momentum (N)	Work done (N-m)	Kinetic energy (N-m)
3.0	50.7/203	1.5	14.8	12.5
6.35	21.7/686	1.4	12.5	11.4
6.35	50.7/228	2.9	12.5	11.3
12.7	50.7/262	3.8	12.5	13.2

Table 5. Impact energies on the non-delaminated side for the delaminated specimens.

Delamination length(mm)	Weight(N)/ Height(mm)	Momentum (N-m)	Work done (N-m)	Kinetic energy (N-m)
152.4	21.7/25	0.7	0.4	0.3
101.6	21.7/51	0.4	0.9	0.8
50.8	21.7/203	0.8	4.2	3.5
25.4	21.7/660	1.8	15.1	13.0
12.7	21.7/838	2.0	19.4	16.5

Table 6. Impact response on the delaminated side for the delaminated specimens.

Delamination length(mm)	Weight(N)/ Height(mm)	Momentum (N-m)	Work done (N-m)	Kinetic energy (N-m)
152.4	21.7/25	0.9	0.8	0.5
101.6	21.7/51	0.7	1.2	0.5
50.8	21.7/203	0.7	1.8	1.5
25.4	21.7/660	1.5	10.4	11.7
12.7	21.7/838	1.2	11.4	10.4

the work done and the kinetic energy for the delaminated specimens were in magnitude for the 50.8mm, 101.6mm, and 152.4mm delamination lengths as compared to the non-delaminated specimen. The work done and the kinetic energy for the 12.7mm and 25.4mm delaminated specimens impacted on the non-delaminated side was greater than those of the non-delaminated specimens. This goes against all reasoning, but the same phenomenon has been reported in experiments for the specimen with intermittent interlaminar bonding (Jea and Felbeck, 1980), and analysis for the delaminated sandwich beams (Hwu and Hu, 1992). Overall, the non-delaminated specimens generally withstood greater impact energies, and the resulting forces and strains before failure, than did the delaminated specimens. As the core mate-

rial carries the major portion of the shear stresses that develop during the impact loading, any discontinuity or abrupt irregularity such as a large scale delamination area becomes a crack initiation site, and failure by core shear results. Realizing that the most prevalent damage of foam cored sandwich composites subjected to low energy impact occurs at the interface between faceplate and core, we expect the impact on the delaminated side to result in failure energies, and the resulting forces and strains to be less than those for impact on the non-delaminated side.

6. Conclusions

The focus of this study is an experimental investigation of damage tolerance of the foam cored symmetric sandwich composites subjected to low energy impact. The response of the impact is relatively complex. From this study, the following conclusions can be obtained.

(1) The force history information may be used to develop equations for the momentum imparted to the specimen, the work done on the specimen, and the kinetic energy, which are the more prominent factors in failure. As the core thickness of the non-delaminated specimens is increased, the maximum impact force at failure increases, but the kinetic energy transferred remains relatively constant.

(2) No specimens displayed any visual signs of damage, including sharp drops in the impact force or strain versus time curves, at any impact energy below the level caused which catastrophic failure.

(3) The maximum force and kinetic energy absorbed in impact are much less for 50.8mm, 101.6mm, and 152.4mm delaminated specimens than those for the non-delaminated specimens. The values are almost equal for the 25.4mm delaminated case, but the 12.7mm delaminated specimen impacted on the non-delaminated side absorbs more kinetic energy before failure than does the non-delaminated specimen. For delaminated specimens, failure occurs at lower energies with impact on the delaminated side than with impact on the non-delaminated side.

References

Carlyle, J. D. and Adler, W. F., 1984, "Damage Tolerance Assessment Procedures for Composite Materials and Components," Presented at the JANNAF Composite Motor Case Subcommittee/ Structures and Mechanical Behavior Subcommittee Joint Meeting, Pasadena, California.

Crane. R. M. and Juska, T. D., 1989, "Instrumented Impact Testing of Composite Materials," David Taylor Research Center, DTRC-SME-88/73.

Hwu, C. and Hu, J. S., 1992, "Buckling and Postbuckling of Delaminated Composite Sandwich Beams," *AIAA Journal,* Vol. 30, pp. 1901 ~1909.

Jea, L. C. and Felbeck, D. K., 1980, "Increased Fracture Toughness of Graphite-Epoxy Composites Through Intermittent Interlaminar Bonding," *Journal of Composite Materials,* Vol. 14, pp. 245 ~259.

Johnson, A. F. and Sims, G. D., 1986, "Mechanical Properties and Design of Sandwich Materials," *Composites,* Vol. 17, pp. 321~328.

Kim, C. and Jun, E., 1992, "Impact Resistance of Composite Laminated Sandwich Plates," *Journal of Composite Materials,* Vol. 26, pp. 2247 ~2261.

Nemes, J. A. and Simmonds, K. E., 1992, "Low-Velocity Impact Response of Foam-Core Sandwich Composites," *Journal of Composite Materials,* Vol. 26, pp. 500~518.

Sjoblöm, P. O., Hartness, J. T. and Cordell, T. M., 1988, "On Low-Velocity Impact Testing of Composite Materials," *Journal of Composite Materials,* Vol. 22, pp. 30~52.